https://doi.org/10.5194/egusphere-2026-6574
Preprint. Discussion started: 6 November 2026
© Author(s) 2026. CC BY 4.0 License.

Online Measurements Reveal Contrasting Particle-Bound Reactive Oxygen Species and Chemical Composition in Emissions from Six Residential Solid Fuels

Lu Lei[1*], Shan Wang[1], Jonas Enarsson[2], Jian Zhao[3], David Nganga[1], Ying Li[4], William Smith[4], Kirsten N. Fossum[1], Aneta Wierzbicka[2], Axel Eriksson[2], Chunshui Lin[1,5], Darius Ceburnis[1], John Wenger[6], Stig Hellebust[6], Colin O'Dowd[1], and Jurgita Ovadnevaite[1*]

[1]The Ryan Institute Centre for Climate & Air Pollution Studies, School of Natural Sciences, Physics, University of Galway, Galway, H91 CF50, Ireland

[2]Ergonomics and Aerosol Technology, Lund University, Lund, Sweden

[3]Institute for Atmospheric and Earth System Research/Physics, Faculty of Science, University of Helsinki, Helsinki, 00014, Finland

[4]School of Mechanical and Materials Engineering, University College Dublin, Dublin, Ireland

[5]Chemistry and Physics, Institute of Earth Environment, Chinese Academy of Sciences, Xi'an, 710061, China

[6]School of Chemistry and Sustainability Institute, University College Cork, Cork, Ireland

Correspondence to: Lu Lei (lu.lei@universityofgalway.ie) and Jurgita Ovadnevaite (jurgita.ovadnevaite@universityofgalway.ie)

Abstract: Residential solid fuel combustion is an important source of atmospheric particulate matter (PM), yet source-dependent characteristics in particle-bound reactive oxygen species (ROS) and their chemical drivers remain poorly constrained. Here, we combined online ROS measurements using a Particle Into Nitroxide Quencher with high-resolution aerosol mass spectrometry to systematically characterize real-time emissions from six residential solid fuels under realistic residential burning conditions. Distinct fuel-dependent chemical signatures were identified: wood-based fuels showed high contributions from oxygen-containing organic ions (O/C = 0.61-0.63), whereas manufactured coals were dominated by hydrocarbon-rich fragments and stronger polycyclic aromatic hydrocarbon (PAH)-related signatures (5-7% of OA). Importantly, these PAH-related ions were strongly associated with mass-normalized ROS (ROS_m) across the six fuels (r^2 = 0.98 for burn-averaged data), while weaker positive time-resolved correlations suggested additional influences from particle chemistry and combustion conditions. Consistently, manufactured coals exhibited substantially higher ROS_m than wood-based fuels and peat (2.2-2.9 vs. 0.2-0.6 pmol BPEAnit-Me equivalents μg^{-1}), together with greater within-burn variability. However, air-volume-normalized ROS (ROS_v) revealed contrasting pathways to elevated ROS burden: coals exhibited the highest ROS_v (140.1-305.4 pmol m^{-3}) driven by their high intrinsic ROS activity, whereas peat reached similarly elevated levels (107.5 pmol m^{-3}) primarily because of its high PM loading. Overall, by linking real-time particle-bound ROS with aerosol chemistry across six solid fuels, this study reveals distinct chemical and mass-loading contributions to ROS burdens, providing a basis for interpreting source-dependent oxidative characteristics of atmospheric combustion aerosols.

https://doi.org/10.5194/egusphere-2026-6574
Preprint. Discussion started: 6 November 2026
© Author(s) 2026. CC BY 4.0 License.

1 Introduction

Exposure to atmospheric particulate matter (PM) is associated with a wide range of adverse respiratory, cardiovascular and mental health effects (Pope and Dockery, 2012; Liu et al., 2019; Nobile et al., 2023). However, PM mass concentration alone does not adequately capture the variations in PM physicochemical properties, e.g., particle size, surface properties, and chemical composition, all of which may influence particle toxicity and associated health outcomes (Kelly and Fussell, 2012; He and Zhang, 2022; Tassel et al., 2025). Oxidative stress, arising from the imbalance between reactive oxygen species (ROS) and biological antioxidant defences, has been considered an important mechanism linking PM exposure to adverse health effects (Moller et al., 2010; Liu and Schauer, 2025). PM can contribute to excess oxidative stress through direct introduction of pre-existing ROS carried on or within inhaled particles, commonly termed particle-bound ROS, which represents reactive species already associated with airborne particles, including radicals and non-radical oxidants with widely varying reactivities and lifetimes (Simões et al., 2021; Carlino et al., 2023; Elkaee et al., 2025). In contrast, oxidative potential (OP) describes the capacity of PM to drive oxidative reactions, including ROS generation and antioxidant depletion, and is frequently investigated as a complementary indicator of particle toxicity (Bates et al., 2019; Liu and Schauer, 2025). Particle-bound ROS and OP therefore represent distinct but complementary aspects of particle oxidative properties, both of which have attracted increasing attention as health-relevant metrics for assessing PM-associated health effects.

Despite growing interest in OP and particle-bound ROS, their accurate quantification remains challenging due to the chemical diversity of redox-active aerosol components and assay-dependent sensitivity, as well as the high reactivity and short lifetimes of certain particle-bound ROS species (Bates et al., 2019; Dominutti et al., 2023; Carlino et al., 2023). Most established approaches rely on filter collection followed by offline extraction and analysis using assays such as dithiothreitol (DTT) (Cho et al., 2005; Rinaldi et al., 2024), ascorbic acid, glutathione (Godri et al., 2011; Fang et al., 2016), or fluorescent ROS probes (Dominutti et al., 2023; Vernocchi et al., 2025). Such approaches are valuable for integrated exposure measurements but are labour-intensive and typically provide low temporal resolutions of hours to days. More importantly for particle-bound ROS, some reactive species have lifetimes of only a few minutes, making them susceptible to losses during prolonged sample collection, storage, and extraction. For instance, Fuller et al. (2014) demonstrated that around 80% of ROS in lab-generated organic aerosols decayed within minutes, while Campbell et al. (2025) showed that short-lived components accounted for 60-99% of the measured ROS and OP in several aerosol types, including combustion-generated particles, highlighting their potential underestimation by conventional offline methods.

These limitations have motivated the development of online measurement techniques in recent years. For example, Wragg et al. (2016) developed the Online Particle-bound ROS Instrument, using a 2′,7′-dichlorofluorescin (DCFH)-based fluorescence assay, and demonstrated its application in London, measuring ambient ROS concentrations up to 24 nmol H_2O_2 equivalents m^{-3} at less than 12 min resolution. Zhou et al. (2018a) applied an improved DCFH-based analyzer to ambient and wood-combustion aerosols, identifying substantial ROS losses during offline analysis (60 ± 20%). Using an automated online DTT system, Puthussery et al. (2018) obtained hourly ambient OP measurements, revealing clear diurnal variations and a fourfold increase during a fireworks pollution episode. However, these existing online ROS systems span temporal resolutions from several minutes to hours, and some remain too slow to resolve rapid changes in strongly dynamic sources such as combustion. In addition, many systems rely on aqueous particle collection or extraction and may incompletely capture water-

https://doi.org/10.5194/egusphere-2026-6574
Preprint. Discussion started: 6 November 2026
© Author(s) 2026. CC BY 4.0 License.

insoluble particle material, which can also be an important contributor to aerosol toxicity (Verma et al., 2012; Gao et al., 2017). The Particle Into Nitroxide Quencher (PINQ) was developed to address several of these limitations by combining rapid particle collection with the profluorescent nitroxide probe 9,10-bis(phenylethynyl)anthracene nitroxide (BPEAnit), enabling sensitive, highly time-resolved measurements of particle-bound ROS and improved representation of insoluble particle components (Brown et al., 2019b). In laboratory chamber experiments, PINQ measurements revealed both short- and long-lived ROS fractions in primary cigarette smoke (Brown et al., 2020). Its application during an ambient campaign in Guangzhou further demonstrated its capability to capture short-term ROS variability alongside real-time aerosol chemical measurements (Brown et al., 2019a).

Residential heating, particularly solid fuel combustion, remains an important source of wintertime air pollution worldwide despite ongoing efforts to transition towards cleaner heating alternatives. In Ireland, residential combustion of peat, wood, and coal has been identified as a major contributor to ambient submicron particulate matter (PM_1, particles with an aerodynamic diameter smaller than 1 μm), particularly during the heating season (Kourtchev et al., 2011; Dall'osto et al., 2013; Lin et al., 2018; Ovadnevaite et al., 2021; Lei et al., 2026). Similarly, domestic combustion of solid biomass and fossil fuels continues to affect air quality across Europe (Denier Van Der Gon et al., 2015) and other regions (Chowdhury et al., 2023; Yun et al., 2020). Beyond its significant contribution to ambient PM mass loading, growing evidence also identifies solid fuel combustion as an important source of ambient aerosol oxidative activity. For example, Rinaldi et al. (2024) attributed the water-soluble DTT-based OP associated with organic aerosol sources in Birr, Ireland, predominantly to residential wood (87%) and peat (13%) combustion. At the European scale, Daellenbach et al. (2020) identified secondary organic aerosols largely originating from residential biomass burning as important contributors to fine-mode OP. Similarly, Luo et al. (2024) reported that biomass burning and coal combustion together accounted for over 52% of the methanol-soluble DTT-based OP during the heating season in Xi'an, China. However, residential solid fuels encompass a wide range of chemically and physically distinct materials. Differences in fuel composition, moisture content, and combustion characteristics can substantially influence particulate emissions and aerosol chemical composition, with potential implications for their health-related properties (Lin et al., 2017; Price-Allison et al., 2019; Trubetskaya et al., 2021). Establishing source-specific ROS characteristics through controlled combustion experiments, particularly alongside detailed aerosol chemical measurements, is therefore important for understanding the potential contributions of individual fuels to ambient particle-bound ROS and providing an experimental basis for future ROS source attribution.

In this study, we combined real-time PINQ measurements with high-resolution aerosol mass spectrometry and collocated online instruments to investigate emissions from six commonly used residential solid fuels burned under controlled open-fireplace conditions representative of real-world residential heating practices. We characterized the fuel-dependent chemical composition of the emitted particles and quantify both mass-normalized and air-volume-normalized particle-bound ROS. By resolving ROS and aerosol chemistry simultaneously throughout individual combustion experiments, we further examined within-burn variability and the chemical characteristics associated with particle-bound ROS activity. This combined approach allows us to explore whether fuels producing chemically distinct particles also differ in their intrinsic ROS activity, and how particle-specific ROS activity and particle loading together shape the particle-bound ROS concentration of residential solid-fuel emissions.

https://doi.org/10.5194/egusphere-2026-6574
Preprint. Discussion started: 6 November 2026
© Author(s) 2026. CC BY 4.0 License.

2 Experimental Methods

2.1 Solid fuels and combustion protocol

Six solid fuels commonly used for residential heating in Ireland were investigated in the combustion experiments, including:

- Kiln-dried hardwood (birch, KDHW), with a relatively low moisture content (< 10 wt.%);
- Green softwood (spruce, GSW), which has a relatively high moisture content (> 30 wt.%);
- Wood briquettes (WB), a compressed biomass fuel;
- Sod peat (SP);
- Low-sulfur manufactured coal (LSMC, sulfur content < 2 wt.%); and
- High-sulfur manufactured coal (HSMC, sulfur content > 2 wt.%).

Further details on the physicochemical properties of the six fuels are provided in Table S1, while photographs of each fuel are presented in Fig. S1. All six solid fuels were sourced within Ireland, either directly from local producers or through local suppliers and retailers.

All fuels included in the present study were burned in a custom-built open fireplace with internal dimensions of 60 × 40 × 30 cm (H × L × W), which was designed to represent typical residential open-fire combustion conditions. The fireplace was connected to a dedicated exhaust flue equipped with a downstream extraction system. During combustion, the extraction system was operated to maintain a relatively stable flue draught and a slight negative pressure (-15 to -12 Pa) within the flue relative to the surrounding environment, allowing continuous removal and transport of the combustion emissions. A consistent general combustion protocol was applied to all fuels, with minor fuel-specific adjustments where necessary. Combustion was initiated using 100 g firelighter, while about 500 g of kindling was additionally used for green softwood and wood briquettes, for which stable ignition was more difficult to achieve. The initial fuel load and subsequent refuelling masses were fuel-specific and were determined through preliminary combustion tests, taking into account the dimensions of the fireplace and the combustion characteristics of each fuel. The selected fuel loads were intended to ensure stable combustion throughout the experiment while avoiding an excessive number of refuelling events. Refuelling was carried out only after the preceding fuel load had been entirely consumed and no visible flame remained. Each combustion experiment lasted around 4 h from initial ignition. Overall, the experimental design was intended to reproduce realistic residential heating conditions as closely as possible, while maintaining controlled and consistent combustion procedures across the different fuels.

The measurements presented in this study were part of a broader residential solid fuel combustion campaign. Additional replicate combustion experiments were conducted for the determination of emission factors, including measurements using both the open fireplace and a traditional stove. However, these experiments are outside the scope of the present study and will be presented in different manuscripts. The present work focuses exclusively on the PINQ measurements conducted with the open fireplace. For the PINQ dataset, one independent combustion experiment was performed for each fuel type, except for low-sulfur manufactured coal, for which two independent combustion experiments were conducted.

2.2 Experimental setup and instruments

https://doi.org/10.5194/egusphere-2026-6574
Preprint. Discussion started: 6 November 2026
© Author(s) 2026. CC BY 4.0 License.

The experimental setup used for the combustion experiments is illustrated in Fig. S2. Combustion exhaust was sampled directly from the chimney through a 3/8-inch stainless-steel sampling line. Before reaching the instruments, the sampled flue passed sequentially through a water trap, a $PM_{2.5}$ cyclone, and a Dekati eDiluter Pro (Dekati Ltd., Finland). The eDiluter was typically operated at a dilution ratio of 150. After cooling and dilution, the conditioned emission was distributed to a suite of online instruments for simultaneous characterization of aerosol properties and gaseous species. Aerosol filter samples were also collected for subsequent offline OP analysis, however those results will be presented separately and are not discussed further here.

An eXtended-resolution time-of-flight Aerosol Chemical Speciation Monitor (ToF-ACSM-X, Aerodyne Research Inc., USA) (Nault et al., 2025) was the primary instrument used to characterize the high-resolution non-refractory PM_1 (NR-PM_1) chemical composition, including organic aerosol (OA), sulfate (SO_4), nitrate (NO_3), ammonium (NH_4) and chloride (Cl). A quadrupole Aerosol Chemical Speciation Monitor (Q-ACSM, Aerodyne Research Inc., USA) (Ng et al., 2011) equipped with a $PM_{2.5}$ aerodynamic lens was operated in parallel to provide complementary unit mass resolution measurements of NR-$PM_{2.5}$. Despite their different sampling size ranges, the two ACSMs provided a useful cross-check of the major aerosol components**.** In particular, the OA concentrations measured by the two ACSMs showed good agreement across the seven combustion experiments included in this study (r^2 = 0.98, slope = 0.86), supporting the overall consistency of the measurements. Equivalent black carbon (eBC) mass concentrations were measured using a seven-wavelength Aethalometer (model AE33, Magee Scientific, USA), while particle number size distributions and total number concentrations over the 10-500 nm range were measured using a scanning mobility particle sizer (SMPS, TSI Inc., USA). Gas-phase nitrogen oxides (NOx), sulfur dioxide (SO_2), ozone (O_3), and carbon monoxide (CO) were measured simultaneously using dedicated gas analyzers (Teledyne API models 200A, T100, and T300 for NOx, SO_2, and CO, respectively, and Thermo Scientific model 49i for O_3). Most online measurements were acquired at a time resolution of 1 min to capture the rapid variability of combustion emissions, whereas the SMPS operated at a 5-min resolution because of the time required for a complete particle-size scan.

A Particle Into Nitroxide Quencher (PINQ) was deployed for real-time quantification of particle-bound ROS. The PINQ uses 9,10-bis(phenylethynyl)anthracene-nitroxide (BPEAnit) dissolved in dimethyl sulfoxide (DMSO), typically at a concentration of 4 μM, as a pro-fluorescent probe (Brown et al., 2019b; Enarsson et al., 2026). Upon reaction with a broad range of ROS, BPEAnit is converted into a stable fluorescent derivative, commonly represented by its methyl adduct BPEAnit-Me. The vortex-based particle collector directly captures particles into the liquid probe solution, enabling measurement of particle-bound ROS associated with both water-soluble and water-insoluble particle fractions. The collected particles are rapidly mixed with the BPEAnit solution, after which the reacted liquid is transferred through a flow-through fluorescence cell. In the cell, the sample is excited by a 450 nm laser (Thorlabs, USA) and the resulting fluorescence is detected spectroscopically (Ocean HDX, Ocean Optics, USA). The rapid collection, reaction, and detection procedure enables the measurement of short-lived particle-bound ROS. The fluorescence response is quantified in terms of BPEAnit-Me equivalents, with BPEAnit-Me serving as the calibration standard. Following the combustion experiments, the PINQ was calibrated using a series of BPEAnit-Me standards of known concentrations, from which a fluorescence-concentration calibration curve was established (Fig. S3) and used to convert the measured fluorescence response into BPEAnit-Me-equivalent particle-bound ROS concentrations. The PINQ has previously been applied in both laboratory and

https://doi.org/10.5194/egusphere-2026-6574
Preprint. Discussion started: 6 November 2026
© Author(s) 2026. CC BY 4.0 License.

ambient measurements and has a reported detection limit of 0.08 nmol m^{-3} at a time resolution of 1 min (Brown et al., 2019b).

In this study, the PINQ was operated at a total flow rate of approximately 20 L min^{-1}. Of this total flow, ~ 8 L min^{-1} was drawn from the diluted combustion-emission sampling line to maintain isokinetic sampling, while the remaining 12 L min^{-1} was supplied as particle-free make-up air. The PINQ alternated between particle-containing and gas-phase sampling modes with a HEPA filter, allowing the particle-phase ROS signal to be distinguished from the gas-phase contribution. The effective time resolution of the PINQ measurements was 6 min in the present study, accounting for the switching between the two sampling modes and the time required for the signal to reach equilibrium after each transition. In addition, different from the original PINQ configuration described by Brown et al. (2019b), the PINQ used in the present study was operated in a modified configuration without the condensational growth chamber, with particles collected directly into the BPEAnit solution using the vortex collector, to improve instrument performance and operational stability. Preliminary characterization using sodium chloride particles indicated a size-dependent collection efficiency, increasing from ~50% at 50 nm to 90% at around 90 nm. The particle number size distributions measured during the combustion experiments exhibited peak diameters above 50 nm for all fuels, suggesting that a substantial fraction of the emitted particles fell within a size range where the PINQ exhibited moderate to high collection efficiency. Although smaller particles generally contribute less to PM mass, their contribution to particle-bound ROS remains uncertain because the size distribution of ROS is unknown. Consequently, the lower collection efficiency for smaller particles may introduce additional uncertainty into the reported ROS concentrations.

2.3 Data analysis

The ToF-ACSM-X and Q-ACSM datasets were processed using the standard ACSM data-analysis software packages in Igor Pro (Version 1.6.1.1 for Q-ACSM and version 4.0.2b for ToF-ACSM-X respectively, WaveMetrics, USA). Both instruments were calibrated for ionization efficiency (IE) and relative ionization efficiency (RIE) before and after the combustion experiments. A collection efficiency (CE) of 1 was applied to both ACSM datasets. In addition, high-resolution peak fitting was performed on the ToF-ACSM-X dataset, during which 21 selected polycyclic aromatic hydrocarbon (PAH)-related ions (listed in Table S2) were fitted following established approaches (Dzepina et al., 2007) and quantified as PAH-related concentrations. The elemental ratios of OA, including oxygen-to-carbon (O/C), hydrogen-to-carbon (H/C) and nitrogen-to-carbon (N/C), were calculated from the high-resolution mass spectra using the Improved-Ambient (IA) elemental analysis method described by Canagaratna et al. (2015). Unless otherwise specified, the aerosol chemical composition results presented in this study were primarily derived from the ToF-ACSM-X measurements. eBC mass concentrations were retrieved from the AE33 measurements using a mass absorption cross-section (MAC) of 7.77 m^2 g^{-1} at 880 nm.

The PINQ data were initially processed using custom-built software, in which the fluorescence signal was synchronized with the valve-position record to distinguish between the filtered mode (gas phase only) and the aerosol mode (particles + gas). Following each valve switch, the first 60 s of data were discarded to allow the signal to re-equilibrate before averaging. Background fluorescence was subtracted, and data points affected by bubbles or other obvious artefacts were excluded. The particle-bound ROS signal was obtained by subtracting the filtered-mode signal from the corresponding aerosol-mode signal. The resulting particle-phase signal was further

https://doi.org/10.5194/egusphere-2026-6574
Preprint. Discussion started: 6 November 2026
© Author(s) 2026. CC BY 4.0 License.

processed in Igor Pro and converted, using the BPEAnit-Me calibration and sampling flow information, into air-volume-normalized ROS (ROS_v) and particle-mass-normalized ROS (ROS_m).

All raw datasets underwent quality assurance and quality control, and only measurements that passed the data-quality criteria were retained for subsequent analyses. Measurements with PM_1 mass concentrations below 10 μg m^{-3} were also excluded to avoid large uncertainties in the mass-normalized ROS values at very low particle loadings. This threshold was applied consistently across all datasets to ensure that subsequent analyses were based on the same valid measurement periods. To minimize interference from firelighter emissions during ignition, which were characterized by particularly high eBC concentrations (Lin et al., 2023), the first 10-15 min of each combustion experiment were generally excluded. The exact exclusion period was adjusted for individual burns according to the temporal evolution of the measured eBC concentration.

3 Results and discussion

3.1 Chemical fingerprints of residential solid fuel combustion aerosols

The health-relevant properties of atmospheric aerosols depend not only on particle mass but also strongly on their chemical composition. This is particularly relevant for particle-bound ROS, as different organic and inorganic constituents can differ substantially in their redox activity and ability to generate or stabilize ROS (Elkaee et al., 2025). Therefore, the chemical composition of particles generated from the six solid fuels was first characterized to provide a chemical context for interpreting the variability in particle-bound ROS discussed in the following sections.

Figure 1a shows the average composition of the measured PM_1 mass (PM_1 = NR-PM_1 + eBC) during the combustion experiments. OA was the dominant component for all six fuels, accounting for 67-97% of the PM_1 mass. Particularly high OA fractions were observed for green softwood (97%) and sod peat (96%), whereas kiln-dried hardwood exhibited a substantially larger eBC contribution of 26%. Wood briquettes, low-sulfur and high-sulfur manufactured coal showed intermediate eBC fractions of 10-11%. The strong OA dominance is in good agreement with previous residential solid-fuel combustion studies, where OA constituted approximately 80-90% of particulate emissions from wood and sod peat and remained a major component of coal-derived particles (Lin et al., 2017; Trubetskaya et al., 2021). Fuel moisture might be an important factor contributing to the differences in the relative contributions of OA and eBC among the fuels. As listed in Table S1, green soft wood has the highest moisture content among the six fuels (> 30%), followed by sod peat (16.5%), and they both produced strongly OA-dominated particles with only minor eBC contributions (1-2%) in the present experiments. High fuel moisture can reduce the energy available for fuel heating and oxidation, thereby impairing stable and efficient combustion and favouring the formation of organic-rich particulate emissions (Shen et al., 2013a; Price-Allison et al., 2019). Although the modified combustion efficiency (MCE) could not be calculated directly for the seven burns investigated here because raw CO and CO_2 measurements were unavailable, repeated open fireplace experiments conducted with the same fuels within the broader campaign provide supporting evidence for this interpretation. In those experiments, green softwood and sod peat exhibited the lowest average MCE values, 0.89 ± 0.02 and 0.86 ± 0.05, respectively, compared with 0.93-0.95 for other fuels (Table S1). These observations suggest that the relatively high moisture contents of green softwood and sod peat may have contributed to their lower combustion efficiencies and, consequently, to the OA-rich and eBC-poor particle composition observed here. Similar MCE

https://doi.org/10.5194/egusphere-2026-6574
Preprint. Discussion started: 6 November 2026
© Author(s) 2026. CC BY 4.0 License.

values of 0.82-0.92 have been reported in previous studies of peat combustion, where burning was predominantly characterized by smouldering conditions (Schneider et al., 2024). Nevertheless, other fuel-specific properties and combustion conditions, in addition to fuel moisture, may also have contributed to the observed differences in particle composition, reflecting the complex nature of residential solid fuel combustion.

A further compositional difference was observed for the manufactured coal fuels, which generally exhibited higher sulfate fractions than the other fuels. This feature was particularly pronounced for high-sulfur manufactured coal, where sulfate accounted for 19% of the measured PM_1 mass, compared with about 3% for low-sulfur manufactured coal. The higher sulfate fraction in high-sulfur manufactured coal is attributed to its higher fuel sulfur content (2.2 vs. 1.4 wt.%, Table S1). More broadly, residential coal combustion has been identified as an important direct source of primary particulate sulfate, with sulfate accounting for a substantial fraction of emitted particle mass in source measurements (Dai et al., 2019). However, the substantially larger difference in particulate sulfate between high-sulfur and low-sulfur manufactured coal than in their bulk sulfur contents suggests that fuel sulfur content alone may not fully explain the observed contrast. The fate of sulfur during combustion, including its distribution between gaseous SO_2, particulate sulfate, and ash-retained sulfur, can also be influenced by sulfur speciation, mineral and ash composition, and combustion conditions (Jia et al., 2016; Shen et al., 2021).

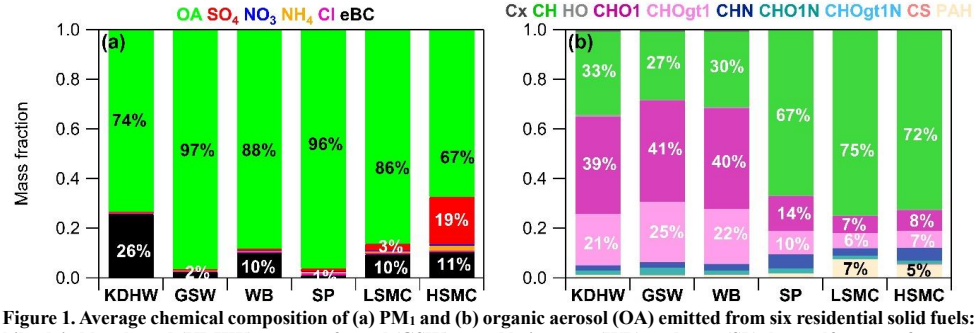


Figure 1. Average chemical composition of (a) PM_1 and (b) organic aerosol (OA) emitted from six residential solid fuels: kiln-dried hardwood (KDHW), green softwood (GSW), wood briquettes (WB), sod peat (SP), low-sulfur manufactured coal (LSMC), and high-sulfur manufactured coal (HSMC).

Much clearer fuel-dependent differences emerged when the organic fraction was examined using the high-resolution measurements from ToF-ACSM-X (Fig. 1b). The three wood-based fuels, kiln-dried hardwood, green softwood and wood briquettes, showed remarkably similar OA signatures and were dominated by oxygen-containing fragment ions. CHO1 ions, i.e., organic fragments containing carbon, hydrogen, and one oxygen atom, accounted for 39-41% of the OA signal, while ions containing more than one oxygen atom (CHOgt1) further contributed 21-25% of the total OA mass. In contrast, these oxygen-containing families accounted for only 7-8% and 6-7%, respectively, of the aerosol mass emitted from the two manufactured coals. The coal-derived OA was instead dominated by CH ions, which contributed 72-75% of the total OA mass. This contrast is consistent with the fundamentally different chemical structures of the parent fuels. Wood consists largely of oxygen-rich biopolymers, particularly cellulose, hemicellulose, and lignin, and their thermal decomposition produces abundant oxygenated organic products (Yang et al., 2007; Shen et al., 2010a). In contrast, progressive coalification removes oxygen-containing functional groups and increases the relative abundance and condensation of aromatic carbon structures (Chen et al., 2012). The elemental composition of the fuels themselves showed a similar contrast, with oxygen contents of 42.3-44.1 wt.% in the wood-based fuels compared with only 2.6-6.9 wt.% in the manufactured

https://doi.org/10.5194/egusphere-2026-6574
Preprint. Discussion started: 6 November 2026
© Author(s) 2026. CC BY 4.0 License.

coals (Table S1). Importantly, the coal-derived OA also exhibited a much stronger aromatic signature, particularly in the PAH-related ions, which represented 5-7% of the OA signal from the two manufactured coals but less than 1% for the other fuels. Consistently, residential coal combustion is well established as an important source of particle-phase PAHs, and coal combustion OA factors measured by high resolution aerosol mass spectrometer have been characterized by strong PAH-related ion signals (Sun et al., 2016). Sod peat exhibited an intermediate chemical signature. CH ions accounted for 67% of the OA signal, substantially higher than for the wood-based fuels but somewhat lower than for the manufactured coals, while oxygen-containing CHO1 and CHOgt1 ions together still accounted for 24%. This intermediate behaviour is chemically plausible given the origin of peat as partially decomposed plant material, i.e., compared with fresh woody biomass, peat contains a larger contribution from aromatic and chemically transformed organic structures, while retaining considerably more oxygen- and nitrogen-containing material than more mature coal.

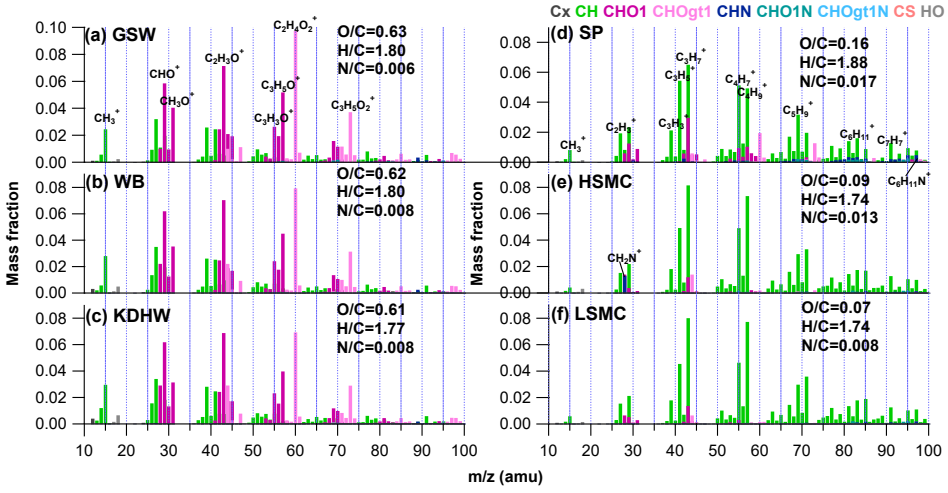


Figure 2. Average high-resolution OA mass spectra obtained during the combustion experiments for each of the six solid fuels. The corresponding average elemental ratios, including oxygen-to-carbon (O/C), hydrogen-to-carbon (H/C), and nitrogen-to-carbon (N/C), are also presented. The most abundant organic fragment ions are labelled.

The differences in OA composition were further illustrated by the average high-resolution organic mass spectra (Fig. 2). The three wood-based fuels displayed prominent oxygenated fragment ions, particularly $C_2H_4O_2^+$ at m/z 60 (6.9-9.7% of the total OA signal) and $C_3H_5O_2^+$ at m/z 73 (2.9-3.7%). These ions are well-established fragments of anhydrosugars such as levoglucosan produced during cellulose pyrolysis and are widely used as characteristic signatures of fresh biomass-burning OA (Weimer et al., 2008; Aiken et al., 2009). Other abundant oxygenated ions, including CHO^+ (5.8-6.2%) and $C_2H_3O^+$ (6.9-7.1%), further distinguished the wood-derived spectra from those of the manufactured coals. In contrast, the mass spectra of manufactured coals were dominated by hydrocarbon fragments and contained much smaller contributions from oxygen-containing ions. They also showed substantially stronger PAH-related ion signals than the other fuels (Fig. S4), providing online mass-spectral evidence of the PAH-rich characteristics of residential coal combustion emissions previously reported in offline studies (Shen et al., 2010b; Shen et al., 2013b). Consistent with these spectral characteristics, the wood-derived OA showed substantially higher O/C ratios (0.61-0.63) than the manufactured-coal OA (0.07-0.09), indicating a considerably greater contribution of oxygen-containing organic material in the wood-burning emissions. The H/C ratios varied over a comparatively narrow range across the six fuels (1.74-1.88) and therefore

https://doi.org/10.5194/egusphere-2026-6574
Preprint. Discussion started: 6 November 2026
© Author(s) 2026. CC BY 4.0 License.

provided much less differentiation among fuel types than O/C. sod peat again exhibited an intermediate chemical signature, with an O/C ratio of 0.16, substantially lower than those of the wood-based fuels but higher than those of the manufactured coals. Notably, sod peat also exhibited noticeable contributions from the two biomass burning marker fragments $C_2H_4O_2^+$ (1.9%) and $C_3H_5O_2^+$ (1.3%), which is also supported by previous observations of levoglucosan in peat-burning emissions (Kourtchev et al., 2011). This result suggests that the presence of these ions in peat emissions may introduce additional uncertainty when using them as tracers to distinguish wood-burning contributions from other combustion sources. In addition, sod peat showed relatively strong contributions from several nitrogen-containing fragments, including CHN-family fragments such as $C_6H_{11}N^+$, and had the highest N/C ratio among the six fuels (0.017 vs. 0.006-0.013). Previous molecular-level measurements have similarly identified abundant CHN- and CHON-containing compounds in peat-burning aerosol (Zhong et al., 2024). The combination of its intermediate O/C and enhanced nitrogen-containing features therefore provides additional chemical information for distinguishing peat-derived OA from the wood- and coal-derived emissions. While there were substantial differences between manufactured coals, sod peat and wood-based fuels, the mass spectra within each fuel class were highly similar. The three wood-based fuel spectra showed tight correlations of $r^2 > 0.95$, while the low-sulfur and high-sulfur manufactured coal profiles were also strongly correlated $r^2 = 0.98$. Sod peat was more distinct from both groups, although its spectrum was more similar to the manufactured coal profiles than to the wood-derived profiles (r^2 = 0.84-0.85 vs. 0.17-0.21). These results indicate that the high-resolution organic spectra provide a strong chemical basis for sorting solid fuel emissions into broad categories but distinguishing fuels within the same class remains a challenge which could be overcome with more source-specific or molecular-level measurements.

Despite the limited number of combustion experiments included in the present ROS dataset, clear and systematic fuel-dependent differences were observed in particle chemical composition, particularly in the high-resolution OA signatures. Importantly, the major compositional patterns identified here were also consistently observed in a separate set of repeated open fireplace combustion experiments using the same fuels, as shown in Fig. S5. Although the absolute contributions of individual components varied slightly among replicate burns, the overall fuel-dependent chemical signatures remained consistent, supporting the representativeness of the patterns observed in the present study. In particular, the oxygen-rich character of wood-derived OA, the hydrocarbon- and PAH-rich signatures of coal-derived OA, and the intermediate characteristics of peat were sufficiently distinct to differentiate the major fuel classes. Importantly, these systematic compositional contrasts provide a direct basis for examining whether differences in ROS activity are associated with specific chemical signatures, while the exact quantitative composition of individual fuels should be considered specific to the combustion conditions of each burn.

3.2 Variability and chemical associations of particle-bound ROS activity

The particle-bound ROS levels of emissions from the six solid fuels were further investigated using real-time PINQ measurements. Figure 3a shows the concentrations of particle-bound ROS across the different fuels, expressed as PM_1-mass-normalized ROS (ROS_m), which represents the intrinsic ROS activity of the emitted particles. The ROS_m values reported here are expressed as pmol BPEAnit-Me equivalents per μg PM_1 and therefore specifically represent the fraction of particle-bound ROS detectable by the BPEAnit assay, rather than the total abundance of all ROS species potentially present in the particles.

https://doi.org/10.5194/egusphere-2026-6574
Preprint. Discussion started: 6 November 2026
© Author(s) 2026. CC BY 4.0 License.

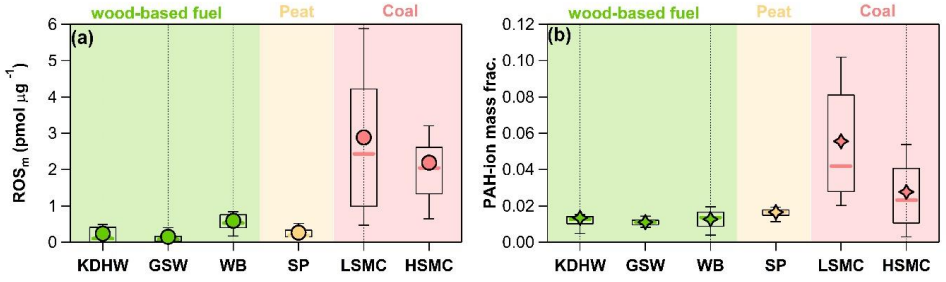


Figure 3. Box plots showing the distributions of (a) mass-normalized particle-bound ROS (ROS_m) and (b) the mass fraction of PAH-related ions in total OA across the six solid fuels. The circles in (a) and diamonds in (b) indicate the mean values, while the horizontal lines indicate the medians. Boxes represent the 25th-75th percentiles, and whiskers extend from the 10th to the 90th percentiles.

Clear differences in ROS_m were observed among the major fuel classes. The manufactured coals exhibited substantially higher ROS_m than both the wood-based fuels and sod peat. More specifically, the average ROS_m reached 2.2-2.9 pmol μg^{-1} for the manufactured coals, whereas the wood-based fuels and sod peat showed much lower values of 0.15-0.59 pmol μg^{-1}. Differences were also observed within the wood-based fuels, specifically, wood briquettes showed the highest average ROS_m (~0.59 pmol μg^{-1}), whereas kiln-dried hardwood and green softwood showed similarly low values (~0.23 and 0.15 pmol μg^{-1}, respectively). The comparable ROS_m levels between kiln-dried hardwood and green softwood is noteworthy given their markedly different moisture contents and the clear influence of moisture on their OA and eBC composition discussed above. This suggests that fuel moisture, although important for combustion behaviour and bulk particle composition, is not by itself a strong predictor of the intrinsic BPEAnit-detectable ROS activity of the emitted particles. In addition, although a recent study has reported potential interference from black carbon in BPEAnit-based ROS measurements, leading to fluorescence suppression and possible underestimation of ROS (Enarsson et al., 2026), no clear indication of such interference was observed in the present dataset.

In addition to their higher average ROS_m, the manufactured coals also exhibited considerably broader ROS_m distributions than the wood-based fuels and sod peat, indicating greater within-burn variability in their intrinsic particle-bound ROS. The pronounced within-burn variability observed here may reflect the dynamic evolution of particle physicochemical properties during combustion. Such changes can be substantial over the course of a single coal burn, particularly in particle loading, size distribution, OA composition, and OA oxidation state (Zhou et al., 2016; Li et al., 2024). Combustion-stage-dependent differences in molecular composition and oxidative potential (Cao et al., 2025) further suggest that evolving particle chemistry may contribute to variations in oxidative characteristics during coal combustion. In the present study, one of the low-sulfur manufactured coal experiments provides a clear example of substantial temporal changes in particle size and chemical composition during combustion. As shown in Fig. S6, PM_1 mass concentrations ranged from 14.7 to 498.9 μg m^{-3} and generally decreased as combustion progressed following each addition of coal (Zhou et al., 2016). Meanwhile, the sulfate mass fraction tended to increase towards the later combustion stages, reaching up to 44% of total PM_1 mass. In contrast, eBC contributed a larger fraction during the early stages, while the PAH-related ion fraction generally declined, varying between 2% and 15%. Concurrent changes were also observed in the OA oxidation state (OSc: -2.0 to -1.5) and particle geometric mean diameter (50-109 nm). Alongside these changes in particle physicochemical properties, ROS_m varied significantly, from near zero to 4.6 pmol μg^{-1}. This case study highlights

https://doi.org/10.5194/egusphere-2026-6574
Preprint. Discussion started: 6 November 2026
© Author(s) 2026. CC BY 4.0 License.

the dynamic nature of coal combustion emissions, demonstrating that considerable within-burn variability in intrinsic particle-bound ROS accompanies the evolving chemical composition and physical characteristics of the emitted particles. The broader ROS_m distributions observed for the manufactured coals therefore suggest that their intrinsic ROS activity may be particularly sensitive to changes occurring during the combustion process. This also has implications for the interpretation of particle-bound ROS measurements. Since ROS_m can vary substantially over an individual burn, measurements obtained over different sampling intervals may place different emphasis on periods with relatively high or low ROS activity, thereby contributing to variability in the reported ROS characteristics. The real-time PINQ measurements used here provide an advantage in this respect by capturing the real-time changes in the ROS_m during individual experiments. Such time-resolved measurements do not replace independent replicate burns, but they enable within-burn variability and transient high-ROS periods to be identified explicitly.

The burn-to-burn variability in ROS_m was also evaluated from the two independent low-sulfur manufactured coal experiments (Fig. S7). A clear difference was observed between the two burns, with average ROS_m values of 4.8 and 1.9 pmol μg^{-1}, respectively. Substantial variability in ROS for residential coal combustion has also been reported in previous studies, with ROS emission factors differing by nearly 20-fold across coal-stove source tests (Luan et al., 2022), highlighting the sensitivity of coal-derived oxidative activity to fuel and combustion conditions. Importantly, however, both low-sulfur manufactured coal experiments exhibited substantially elevated ROS_m relative to the wood-based fuels and sod peat. The repeat experiment therefore supports the broader conclusion that manufactured-coal particles possess higher intrinsic ROS activity under the conditions investigated here, while also demonstrating that the absolute magnitude of ROS_m can vary considerably between individual burns. The repeated low-sulfur manufactured coal experiment also indicates that a systematic difference in ROS_m between low-sulfur and high-sulfur manufactured coal cannot be established from the present dataset, since the second low-sulfur manufactured coal burn showed ROS_m values comparable to high-sulfur manufactured coal (1.9 vs. 2.2 pmol μg^{-1}). This finding is also in line with the highly similar OA composition of the two manufactured coals, as demonstrated in Section 3.1. Although high-sulfur manufactured coal contained a substantially larger sulfate fraction than low-sulfur manufactured coal, major inorganic ions such as sulfate are generally not considered dominant direct contributors to particle-bound ROS activity (Zhou et al., 2018a; Bates et al., 2019). The comparable ROS_m of the two manufactured coals therefore further points to the organic fraction as a more relevant chemical basis for their similar intrinsic ROS characteristics.

To explore the chemical characteristics associated with ROS_m, the burn-averaged ROS levels were compared with major compositional and OA metrics measured during the combustion experiments. Among all the chemical species, the PAH-related ion mass fraction exhibited a highly similar fuel-dependent pattern to that of ROS_m (Fig. 3b). Specifically, the average PAH-related fraction in OA was substantially higher for the manufactured coals (2.8-5.6%) than for the wood-based fuels (1.1-1.3%) and sod peat (1.6%), and the coal emissions also exhibited considerably greater within-burn variability. Consistent with these similar fuel-dependent patterns, burn-averaged ROS_m was strongly correlated with the PAH-related ion fraction ($r^2 = 0.98$, $p < 0.001$; Fig. S8a), indicating a strong association between PAH-rich organic emissions and elevated intrinsic particle-bound ROS activity. This finding is consistent with previous ambient studies suggesting that PAHs can serve as useful indicators of particle oxidative activity. For example, Pietrogrande et al. (2022) reported significant associations between particle oxidative potential and total PAHs, indicating that PAHs may serve as markers of broader combustion-derived

https://doi.org/10.5194/egusphere-2026-6574
Preprint. Discussion started: 6 November 2026
© Author(s) 2026. CC BY 4.0 License.

aromatic mixtures containing redox-active species, including oxygenated PAHs and quinone-like compounds. However, a review of elemental-carbon-containing particles highlighted that PAHs, quinones, and other surface organic functionalities may contribute differently to particle oxidative activity, with quinone-type functionalities being particularly important (Liu and Chan, 2022). Therefore, the strong PAH-ROS association observed in our study does not necessarily imply a direct contribution from parent PAHs alone, but may also reflect the presence of co-emitted redox-active organic compounds and more complex chemical influences on particle-bound ROS.

Importantly, the PAH-ROS association was not confined to the burn-averaged level. When the time-resolved measurements from all combustion experiments were included, ROS_m remained positively associated with the PAH-related ion fraction, although the correlation was relatively weaker ($r^2 = 0.52$, Fig. S8b). This suggests that the very strong fuel-level correlation may partly reflect the pronounced compositional contrast between manufactured coal and wood/peat emissions. Nevertheless, a moderate positive relationship was retained when the analysis was restricted to the coal-combustion periods alone ($r^2 = 0.32$), demonstrating that the association was not solely produced by the broad separation between coal and non-coal fuels. The lower r^2 values obtained from the time-resolved measurements further indicate that PAH-related composition alone cannot account for the full temporal variability in ROS_m, and that additional chemical species, combustion conditions, and mixture effects are also likely to contribute.

Atmospheric aging is another important process that can substantially alter the oxidative characteristics of combustion-derived particles. Previous studies have shown that particle-bound ROS can change considerably during atmospheric oxidation, with the ROS content of secondary organic aerosol being related to its oxidation state (Zhou et al., 2018b). The average carbon oxidation state (OSc), commonly approximated as $(2 \times O/C - H/C)$, provides a bulk measure of the degree of oxidation of OA, with higher OSc indicating more oxidized OA (Kroll et al., 2011). Since the absolute OSc differed substantially among fuel types, the analysis was performed using within-burn deviations from the corresponding burn averages, i.e., $\Delta ROS_m = ROS_m - ROS_{m_avg}$ and $\Delta OSc = OSc - OSc_avg$), thereby removing the large between-fuel offsets and focusing specifically on temporal covariation within individual burns. No clear relationship was observed between ΔROS_m and ΔOSc ($r^2 = 0$, Fig. S8c), indicating that changes in bulk OA oxidation state did not explain the temporal evolution of particle-bound ROS in these fresh combustion emissions. This result does not necessarily conflict with previous observations that atmospheric oxidation can enhance particle oxidative activity. For example, aging experiments with residential wood smoke showed that particle-bound ROS in secondary organic aerosol initially increased with increasing SOA oxidation state, although further aging could subsequently lead to a decline in ROS (Zhou et al., 2018b). More generally, oxidative activity appears to depend strongly on the chemical identity of the oxygen-containing functionalities rather than on bulk oxygenation alone (Liu and Chan, 2022). Thus, a bulk metric such as OSc may not resolve the relatively small subset of redox-active organic species that determine particle-bound ROS activity. Taken together, these results indicate that the intrinsic particle-bound ROS activity cannot be explained simply by the overall oxidation state or bulk chemical composition of the particles. Instead, PAH-related organic species showed the strongest and most persistent association with ROS_m, from fuel-averaged differences to time-resolved variations, while the weaker relationships with broader compositional metrics point to the importance of specific redox-active constituents and complex chemical-mixture effects which needs further investigation in future studies.

3.3 Contrasting fuel-dependent patterns in particle mass and ROS concentrations

https://doi.org/10.5194/egusphere-2026-6574
Preprint. Discussion started: 6 November 2026
© Author(s) 2026. CC BY 4.0 License.

While ROS_m characterizes the particle-bound ROS activity per unit particle mass, the air-volume-normalized ROS concentration (ROS_v) also depends on the amount of particulate matter present in the sampled air. Figure 4 therefore compares the measured PM_1 mass concentration and ROS_v across the six fuels during the valid measurement periods. Substantial differences were observed in PM_1 mass concentration, with sod peat and green softwood showing markedly higher mean concentrations of 546.2 and 440.2 μg m^{-3}, respectively, compared with 53.4-106.5 μg m^{-3} for the other four fuels. Sod peat and green softwood also exhibited substantially broader concentration distributions, indicating greater temporal variability in particle loading during combustion. The elevated particle loadings observed for these two fuels are consistent with their less efficient combustion characteristics, which likely indicates greater smouldering contributions than the other fuels. Smouldering and otherwise inefficient combustion generally favour higher particulate emissions because a larger fraction of the fuel carbon escapes complete oxidation. For green softwood, the high fuel moisture likely reduced combustion temperature and MCE, while substantially increasing PM emission factors (Shen et al., 2013a; Price-Allison et al., 2019). Sod peat also has a relatively high moisture content, and its combustion is often characterised by smouldering, which can result in substantial particulate emissions (Wilson et al., 2025). However, it should be noted that the absolute PM_1 concentrations reported here should not be interpreted as fuel-specific emission factors, because they were not normalized to fuel consumption and the effective dilution ratios could not be reconstructed quantitatively throughout the experiments. Nevertheless, the relative fuel-dependent pattern was independently supported by PM emission factors obtained from six repeated open-fireplace combustion experiments using the same fuels (Fig. S9). In these independent experiments, sod peat and green softwood again showed the highest PM emission factors, whereas kiln-dried hardwood, wood briquettes, low-sulfur and high-sulfur manufactured coal were substantially lower and more comparable. The agreement between the two independent datasets therefore supports the representativeness of the broad relative differences in PM_1 loading observed in the present experiments.

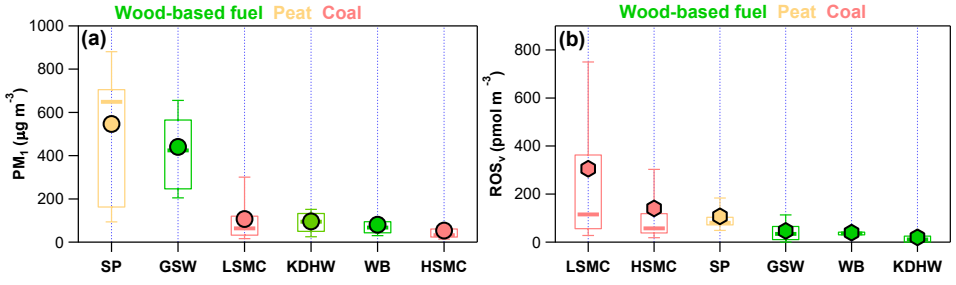


Figure 4. Box plots showing the distributions of (a) PM_1 mass concentration and (b) air-volume-normalized particle-bound ROS (ROS_v) across the six solid fuels. Please note that fuels are arranged in descending order of their respective mean values in each panel. The circles in (a) and hexagons in (b) indicate the mean values, while the horizontal lines indicate the medians. Boxes represent the 25th-75th percentiles, and whiskers extend from the 10th to the 90th percentiles.

In contrast to the PM_1 mass concentration, ROS_v exhibited a clearly different fuel-dependent pattern (Fig. 4b). The highest mean ROS_v was observed for low-sulfur manufactured coal (305.4 pmol m^{-3}), followed by high-sulfur manufactured coal (140.1 pmol m^{-3}), despite their comparatively low PM_1 concentrations (53.4-106.5 μg m^{-3}). This is largely driven by the substantially higher ROS_m of the manufactured-coal particles (2.2-2.9 pmol $μg^{-1}$) and demonstrates that high air-volume-normalized ROS concentrations can arise even when particle mass loading is relatively modest. Sod peat showed the opposite behaviour, although its ROS_m was relatively low (0.28 pmol μg-

https://doi.org/10.5194/egusphere-2026-6574
Preprint. Discussion started: 6 November 2026
© Author(s) 2026. CC BY 4.0 License.



[1]), its much higher PM_1 concentration resulted in a mean ROS_v of 107.5 pmol m^{-3}, comparable to that of high-sulfur manufactured coal. Similarly, green softwood, which exhibited the lowest ROS_m (0.15 pmol μg^{-1}), still showed a moderate ROS_v of 47.0 pmol m^{-3} because of its relatively high particle loading. Conversely, kiln-dried hardwood and wood briquettes combined relatively low PM_1 concentrations with low ROS_m, resulting in the lowest ROS_v levels (19.6-39.3 pmol m^{-3}) among the fuels. These contrasting patterns demonstrate that particle mass loading alone is insufficient to describe the air-volume-based oxidative burden of combustion aerosol, i.e., ROS_v is jointly determined by how much particulate matter is present and how much particle-bound ROS is associated with each unit of particle mass. This distinction is also relevant to ambient aerosol source apportionment. For example, Wang et al. (2020), found that biomass burning contributed the largest fraction of particle mass in Bangkok, whereas fossil-fuel combustion dominated the volume-normalized oxidative potential, demonstrating that source rankings based on particle mass and oxidative activity can differ substantially. Although these studies employed different ROS/OP assays, the common implication is that particle abundance and particle-specific oxidative activity represent complementary dimensions of aerosol exposure. In the present study, the manufactured coals and sod peat illustrate two contrasting pathways to elevated ROS_v: high intrinsic particle-bound ROS activity for the coals, and high particle mass loading for sod peat. This highlights the importance of considering both source-specific particle oxidative characteristics and mass contributions when interpreting ambient particle-bound ROS and assessing the relative importance of different combustion sources.

4 Conclusions

This study provides a systematic investigation of the chemical composition and particle-bound ROS of emissions from six residential solid fuels, combining real-time ROS measurements with high-resolution aerosol chemical characterization under realistic residential heating conditions. Clear fuel-dependent chemical signatures were observed in the emitted particles. The wood-based fuels were characterized by substantially higher contributions from oxygen-containing organic fragment ions and higher O/C ratios (0.61-0.63), whereas the manufactured coals exhibited much more hydrocarbon-rich fragmentation patterns, stronger PAH-related signatures (5-7% of total OA mass), and enhanced sulfate contributions (3-19% of total PM_1 mass). Sod peat showed an intermediate but compositionally distinct chemical profile, including elevated contributions from N-containing ions. These distinct high-resolution chemical signatures can therefore provide experimentally derived anchors for better distinguishing residential solid fuel combustion sources and supporting atmospheric aerosol source apportionment.

Pronounced differences were also observed in the mass-normalized particle-bound ROS activity (ROS_m). The manufactured coals exhibited substantially higher ROS_m than the wood-based fuels and sod peat (2.2-2.9 vs. 0.2-0.6 pmol BPEAnit-Me equivalents μg^{-1} PM_1), indicating substantially greater intrinsic particle-bound ROS activity. Considerable temporal variability in ROS_m was also observed within individual coal burns, indicating that the oxidative characteristics of freshly emitted particles can evolve substantially over the course of a single combustion event. The PAH-related ion fraction was found to be strongly associated with ROS_m across fuels (r^2 = 0.98 for burn-averaged data), with positive but weaker relationships in time-resolved measurements (r^2 = 0.52 overall and 0.32 for coals alone). This suggests that PAH-related composition may serve as an important indicator of fuel-dependent ROS activity. However, the weaker time-resolved relationships indicate that PAH-related composition alone cannot fully explain the temporal variability in ROS_m, highlighting the potential contributions of other redox-active organic constituents, combustion conditions, and matrix effects.

https://doi.org/10.5194/egusphere-2026-6574
Preprint. Discussion started: 6 November 2026
© Author(s) 2026. CC BY 4.0 License.

Interestingly, when intrinsic ROS activity was considered together with particle mass loading, a different fuel-dependent pattern emerged. The manufactured coals showed the highest average ROS_v at 140.1-305.4 pmol (BPEAnit-Me equivalents) m^{-3}, despite their comparatively modest PM_1 mass concentrations (53.4-106.5 µg m^{-3}), mainly driven by their substantially higher ROS_m. In contrast, sod peat reached a similarly notable ROS_v (107.5 pmol m^{-3}) despite its relatively low ROS_m, driven instead by its much higher particle mass loading (546.2 µg m^{-3}). These contrasting behaviours demonstrate that elevated particle-bound ROS concentrations can arise through different pathways, i.e., high particle-specific ROS activity, high particle mass loading, or a combination of both. Therefore, PM mass alone may not adequately characterize the oxidative burden associated with residential solid-fuel combustion. A more complete assessment should consider both the amount of particulate matter emitted and the intrinsic oxidative characteristics of the particles.

Overall, integrating real-time ROS measurements with detailed aerosol chemical characterization provides new insights into fuel-specific chemical fingerprints and temporal variability in particle-bound ROS during combustion, offering valuable information for identifying combustion sources and chemical signatures associated with enhanced ROS activity. The pronounced temporal variability further highlights the value of online measurements for capturing rapidly evolving particle oxidative characteristics. However, as BPEAnit detects only a fraction of particle-bound ROS, combining online PINQ measurements with complementary offline OP assays and alternative ROS probes will be important for a more comprehensive characterization of the oxidative properties of atmospheric aerosols.

Data availability

The data supporting the findings of this study will be made publicly available on Zenodo upon acceptance of the manuscript (https://doi.org/10.5281/zenodo.23394088).

Competing interests.

At least one of the (co-)authors is a member of the editorial board of Atmospheric Chemistry and Physics. The authors have no other competing interests to declare.

Author contributions.

LL, SW, JZ, YL, WS and JO designed the experiments. LL, SW, JZ and YL carried out the measurements. LL, SW and YL performed the data analysis. JE, KNF, DN, CL, AW, AE, JW and SH provided technical support. LL prepared the manuscript with contributions from all co-authors. JO supervised this study.

Acknowledgement.

This publication has emanated from research funded by Taighde Éireann – Research Ireland under Grant number [22/FFP-A/10611]. The research also received funding from European Union's Horizon Europe Research and Innovation programme under HORIZON-CL5-2022-D1-02 (grant no. 101081430 – PARIS). Jian Zhao thanks Research Council of Finland (grant no. 1363283) and University of Helsinki (grant 70996217) for financial support. We sincerely thank John Gahan (Technical Officer, University College Dublin), the staff of the Physics

https://doi.org/10.5194/egusphere-2026-6574
Preprint. Discussion started: 6 November 2026
© Author(s) 2026. CC BY 4.0 License.

Workshop at the University of Galway, Dainius Martuzevičius (Kaunas University of Technology), and Zoran Ristovski (Queensland University of Technology) for their invaluable assistance and continued support throughout the campaign.

References

Aiken, A. C., Salcedo, D., Cubison, M. J., Huffman, J. A., DeCarlo, P. F., Ulbrich, I. M., Docherty, K. S., Sueper, D., Kimmel, J. R., Worsnop, D. R., Trimborn, A., Northway, M., Stone, E. A., Schauer, J. J., Volkamer, R. M., Fortner, E., de Foy, B., Wang, J., Laskin, A., Shutthanandan, V., Zheng, J., Zhang, R., Gaffney, J., Marley, N. A., Paredes-Miranda, G., Arnott, W. P., Molina, L. T., Sosa, G., and and Jimenez, J. L.: Mexico City aerosol analysis during MILAGRO using high resolution aerosol mass spectrometry at the urban supersite (T0) – Part 1: Fine particle composition and organic source apportionment, Atmospheric Chemistry and Physics, 9, 6633–6653, https://doi.org/10.5194/acp-9-6633-2009, 2009., 2009.

Bates, J. T., Fang, T., Verma, V., Zeng, L., Weber, R. J., Tolbert, P. E., Abrams, J. Y., Sarnat, S. E., Klein, M., Mulholland, J. A., and Russell, A. G.: Review of Acellular Assays of Ambient Particulate Matter Oxidative Potential: Methods and Relationships with Composition, Sources, and Health Effects, Environmental Science & Technology, 53, 4003-4019, https://doi.org/10.1021/acs.est.8b03430, 2019.

Brown, R., Stevanovic, S., Brown, Z., Cai, M., Zhou, S., Song, W., Wang, X., Miljevic, B., Zhao, J., Bottle, S., and Ristovski, Z.: Application of a Fluorescent Probe for the Online Measurement of PM-Bound Reactive Oxygen Species in Chamber and Ambient Studies, Sensors (Basel), 19, https://doi.org/10.3390/s19204564, 2019a.

Brown, R. A., Stevanovic, S., Bottle, S., and Ristovski, Z. D.: An instrument for the rapid quantification of PM-bound ROS: the Particle Into Nitroxide Quencher (PINQ), Atmospheric Measurement Techniques, 12, 2387-2401, https://doi.org/10.5194/amt-12-2387-2019, 2019b.

Brown, R. A., Stevanovic, S., Bottle, S., Wang, H., Hu, Z., Wu, C., Wang, B., and Ristovski, Z.: Relationship between Atmospheric PM-Bound Reactive Oxygen Species, Their Half-Lives, and Regulated Pollutants: Investigation and Preliminary Model, Environ Sci Technol, 54, 4995-5002, https://doi.org/10.1021/acs.est.9b06643, 2020.

Campbell, S. J., Utinger, B., Barth, A., Leni, Z., Zhang, Z.-H., Resch, J., Li, K., Steimer, S. S., Banach, C., Gfeller, B., Wragg, F. P. H., Westwood, J., Wolfer, K., Bukowiecki, N., Ihalainen, M., Yli-Pirilä, P., Somero, M., Kortelainen, M., Louhisalmi, J., Sklorz, M., Czech, H., di Bucchianico, S., Streibel, T., Delaval, M. N., Ruger, C., Baumlin, N., Salathe, M., Fang, Z., Pardo, M., D'Aronco, S., Giorio, C., Shi, Z., Harrison, R. M., Green, D. C., Kelly, F. J., Rudich, Y., Paulson, S. E., Sippula, O., Zimmermann, R., Geiser, M., and Kalberer, M.: Short-lived reactive components substantially contribute to particulate matter oxidative potential, Science Advances, 11, eadp8100, https://doi.org/10.1126/sciadv.adp8100, 2025.

Canagaratna, M. R., Jimenez, J. L., Kroll, J. H., Chen, Q., Kessler, S. H., Massoli, P., Hildebrandt Ruiz, L., Fortner, E., Williams, L. R., Wilson, K. R., Surratt, J. D., Donahue, N. M., Jayne, J. T., and Worsnop, D. R.: Elemental ratio measurements of organic compounds using aerosol mass spectrometry: characterization, improved calibration, and implications, Atmospheric Chemistry and Physics, 15, 253-272, https://doi.org/10.5194/acp-15-253-2015, 2015.

Cao, T., Li, M., Song, J., Fan, X., Jiang, B., Zhong, Y., Zhang, G., Song, H., and Peng, P.: Comparison of Residential Coal Combustion Brown Carbon Generated during the Initial and Stable Stages: Insights into Their

https://doi.org/10.5194/egusphere-2026-6574
Preprint. Discussion started: 6 November 2026
© Author(s) 2026. CC BY 4.0 License.

Molecular Composition, Optical Properties, and Oxidative Potential, Environ Sci Technol, 59, 26626-26637, https://doi.org/10.1021/acs.est.5c09367, 2025.

Carlino, A., Romano, M. P., Lionetto, M. G., Contini, D., and Guascito, M. R.: An Overview of the Automated and On-Line Systems to Assess the Oxidative Potential of Particulate Matter, Atmosphere, 14, https://doi.org/10.3390/atmos14020256, 2023.

Chen, Y., Mastalerz, M., and Schimmelmann, A.: Characterization of chemical functional groups in macerals across different coal ranks via micro-FTIR spectroscopy, International Journal of Coal Geology, 104, 22-33, https://doi.org/10.1016/j.coal.2012.09.001, 2012.

Cho, A. K., Sioutas, C., Miguel, A. H., Kumagai, Y., Schmitz, D. A., Singh, M., Eiguren-Fernandez, A., and Froines, J. R.: Redox activity of airborne particulate matter at different sites in the Los Angeles Basin, Environmental Research, 99, 40-47, https://doi.org/10.1016/j.envres.2005.01.003, 2005.

Chowdhury, S., Pillarisetti, A., Oberholzer, A., Jetter, J., Mitchell, J., Cappuccilli, E., Aamaas, B., Aunan, K., Pozzer, A., and Alexander, D.: A global review of the state of the evidence of household air pollution's contribution to ambient fine particulate matter and their related health impacts, Environment International, 173, https://doi.org/10.1016/j.envint.2023.107835, 2023.

Daellenbach, K. R., Uzu, G., Jiang, J., Cassagnes, L.-E., Leni, Z., Vlachou, A., Stefenelli, G., Canonaco, F., Weber, S., Segers, A., Kuenen, J. J. P., Schaap, M., Favez, O., Albinet, A., Aksoyoglu, S., Dommen, J., Baltensperger, U., Geiser, M., El Haddad, I., Jaffrezo, J.-L., and Prévôt, A. S. H.: Sources of particulate-matter air pollution and its oxidative potential in Europe, Nature, 587, 414-419, https://doi.org/10.1038/s41586-020-2902-8, 2020.

Dai, Q., Bi, X., Song, W., Li, T., Liu, B., Ding, J., Xu, J., Song, C., Yang, N., Schulze, B. C., Zhang, Y., Feng, Y., and Hopke, P. K.: Residential coal combustion as a source of primary sulfate in Xi'an, China, Atmospheric Environment, 196, 66-76, https://doi.org/10.1016/j.atmosenv.2018.10.002, 2019.

Dall'Osto, M., Ovadnevaite, J., Ceburnis, D., Martin, D., Healy, R. M., O'Connor, I. P., Kourtchev, I., Sodeau, J. R., Wenger, J. C., and O'Dowd, C.: Characterization of urban aerosol in Cork city (Ireland) using aerosol mass spectrometry, Atmospheric Chemistry and Physics, 13, 4997-5015, https://doi.org/10.5194/acp-13-4997-2013, 2013.

Denier van der Gon, H. A. C., Bergström, R., Fountoukis, C., Johansson, C., Pandis, S. N., Simpson, D., and Visschedijk, A. J. H.: Particulate emissions from residential wood combustion in Europe – revised estimates and an evaluation, Atmospheric Chemistry and Physics, 15, 6503-6519, https://doi.org/10.5194/acp-15-6503-2015, 2015.

Dominutti, P. A., Borlaza, L. J. S., Sauvain, J.-J., Ngoc Thuy, V. D., Houdier, S., Suarez, G., Jaffrezo, J.-L., Tobin, S., Trébuchon, C., Socquet, S., Moussu, E., Mary, G., and Uzu, G.: Source apportionment of oxidative potential depends on the choice of the assay: insights into 5 protocols comparison and implications for mitigation measures, Environmental Science: Atmospheres, 3, 1497-1512, https://doi.org/10.1039/d3ea00007a, 2023.

Dzepina, K., Arey, J., Marr, L. C., Worsnop, D. R., Salcedo, D., Zhang, Q., Onasch, T. B., Molina, L. T., Molina, M. J., and Jimenez, J. L.: Detection of particle-phase polycyclic aromatic hydrocarbons in Mexico City using an aerosol mass spectrometer, Int. J. Mass Spectrom., 263, 152-170, https://doi.org/10.1016/j.ijms.2007.01.010, 2007.

Elkaee, S., Miljevic, B., Stevanovic, S., Wang, R., Wang, H., and Ristovski, Z. D.: Online Monitoring of Particle-Bound Reactive Oxygen Species (ROS) and Oxidative Potential (OP) in a Changing Atmosphere: a Review, ACS ES&T Air, 2, 2753-2775, https://doi.org/10.1021/acsestair.5c00261, 2025.

https://doi.org/10.5194/egusphere-2026-6574
Preprint. Discussion started: 6 November 2026
© Author(s) 2026. CC BY 4.0 License.

Enarsson, J., Malmborg, V., Miljevic, B., Eriksson, A., Wang, H., Ristovski, Z., and Wierzbicka, A.: Interference from carbonaceous particles in reactive oxygen species measurements: A case study with Printex 90 and BPEAnit, EGUsphere, 2026, 1-19, https://doi.org/10.5194/egusphere-2026-3807, 2026.

Fang, T., Verma, V., Bates, J. T., Abrams, J., Klein, M., Strickland, M. J., Sarnat, S. E., Chang, H. H., Mulholland, J. A., Tolbert, P. E., Russell, A. G., and Weber, R. J.: Oxidative potential of ambient water-soluble PM_{2.5} in the southeastern United States: contrasts in sources and health associations between ascorbic acid (AA) and dithiothreitol (DTT) assays, Atmospheric Chemistry and Physics, 16, 3865-3879, https://doi.org/10.5194/acp-16-3865-2016, 2016.

Fuller, S. J., Wragg, F. P. H., Nutter, J., and Kalberer, M.: Comparison of on-line and off-line methods to quantify reactive oxygen species (ROS) in atmospheric aerosols, Atmospheric Environment, 92, 97-103, https://doi.org/10.1016/j.atmosenv.2014.04.006, 2014.

Gao, D., Fang, T., Verma, V., Zeng, L., and Weber, R. J.: A method for measuring total aerosol oxidative potential (OP) with the dithiothreitol (DTT) assay and comparisons between an urban and roadside site of water-soluble and total OP, Atmospheric Measurement Techniques, 10, 2821-2835, https://doi.org/10.5194/amt-10-2821-2017, 2017.

Godri, K. J., Harrison, R. M., Evans, T., Baker, T., Dunster, C., Mudway, I. S., and Kelly, F. J.: Increased oxidative burden associated with traffic component of ambient particulate matter at roadside and urban background schools sites in London, PLoS One, 6, e21961, https://doi.org/10.1371/journal.pone.0021961, 2011.

He, L. and Zhang, J.: Particulate matter (PM) oxidative potential: Measurement methods and links to PM physicochemical characteristics and health effects, Critical Reviews in Environmental Science and Technology, 53, 177-197, https://doi.org/10.1080/10643389.2022.2050148, 2022.

Jia, X., Wang, Q., Cheng, L., Han, L., Ye, C., Fang, M., Luo, Z., and Cen, K.: Sulfur Behavior of Coal and Ash during Coal Pyrolysis Combined with Combustion, Energy & Fuels, 30, 9589-9595, https://doi.org/10.1021/acs.energyfuels.6b01619, 2016.

Kelly, F. J. and Fussell, J. C.: Size, source and chemical composition as determinants of toxicity attributable to ambient particulate matter, Atmospheric Environment, 60, 504-526, https://doi.org/10.1016/j.atmosenv.2012.06.039, 2012.

Kourtchev, I., Hellebust, S., Bell, J. M., O'Connor, I. P., Healy, R. M., Allanic, A., Healy, D., Wenger, J. C., and Sodeau, J. R.: The use of polar organic compounds to estimate the contribution of domestic solid fuel combustion and biogenic sources to ambient levels of organic carbon and PM2.5 in Cork Harbour, Ireland, Sci Total Environ, 409, 2143-2155, https://doi.org/10.1016/j.scitotenv.2011.02.027, 2011.

Kroll, J. H., Donahue, N. M., Jimenez, J. L., Kessler, S. H., Canagaratna, M. R., Wilson, K. R., Altieri, K. E., Mazzoleni, L. R., Wozniak, A. S., Bluhm, H., Mysak, E. R., Smith, J. D., Kolb, C. E., and Worsnop, D. R.: Carbon oxidation state as a metric for describing the chemistry of atmospheric organic aerosol, Nature Chemistry, 3, 133-139, https://doi.org/10.1038/nchem.948, 2011.

Lei, L., Xu, W., Lin, C., Fossum, K. N., Ceburnis, D., Gallagher, J., O'Dowd, C., and Ovadnevaite, J.: Measurement report: Evolving sources and composition of urban submicron aerosols in Dublin: impacts of emission reductions and transboundary transport, Atmos. Chem. Phys., 26, 10927-10946, https://doi.org/10.5194/acp-26-10927-2026, 2026.

https://doi.org/10.5194/egusphere-2026-6574
Preprint. Discussion started: 6 November 2026
© Author(s) 2026. CC BY 4.0 License.

Li, S., Liu, D., Jiang, X., Tian, P., Sheng, J., Wu, Y., Hu, K., Bi, K., Li, R., Zhao, D., Huang, M., Kong, S., and Zheng, C.: Dynamic evolution of particulate and gaseous emissions for typical residential coal combustion, Sci Total Environ, 951, 175851, https://doi.org/10.1016/j.scitotenv.2024.175851, 2024.

Lin, C., Ceburnis, D., Hellebust, S., Buckley, P., Wenger, J., Canonaco, F., Prevot, A. S. H., Huang, R. J., O'Dowd, C., and Ovadnevaite, J.: Characterization of Primary Organic Aerosol from Domestic Wood, Peat, and Coal Burning in Ireland, Environmental Science & Technology, 51, 10624-10632, https://doi.org/10.1021/acs.est.7b01926, 2017.

Lin, C., Huang, R.-J., Ceburnis, D., Buckley, P., Preissler, J., Wenger, J., Rinaldi, M., Facchini, M. C., O'Dowd, C., and Ovadnevaite, J.: Extreme air pollution from residential solid fuel burning, Nature Sustainability, 1, 512-517, https://doi.org/10.1038/s41893-018-0125-x, 2018.

Lin, C., Ceburnis, D., Vaishya, A., Trubetskaya, A., Tan, Y., Wang, T., Smith, W., Johnson, R., Xu, W., Monaghan, R. F. D., O'Dowd, C., and Ovadnevaite, J.: Air quality—climate forcing double whammy from domestic firelighters, npj Climate and Atmospheric Science, 6, 101, https://doi.org/10.1038/s41612-023-00427-x, 2023.

Liu, C., Chen, R., Sera, F., Vicedo-Cabrera, A. M., Guo, Y., Tong, S., Coelho, M., Saldiva, P. H. N., Lavigne, E., Matus, P., Valdes Ortega, N., Osorio Garcia, S., Pascal, M., Stafoggia, M., Scortichini, M., Hashizume, M., Honda, Y., Hurtado-Diaz, M., Cruz, J., Nunes, B., Teixeira, J. P., Kim, H., Tobias, A., Iniguez, C., Forsberg, B., Astrom, C., Ragettli, M. S., Guo, Y. L., Chen, B. Y., Bell, M. L., Wright, C. Y., Scovronick, N., Garland, R. M., Milojevic, A., Kysely, J., Urban, A., Orru, H., Indermitte, E., Jaakkola, J. J. K., Ryti, N. R. I., Katsouyanni, K., Analitis, A., Zanobetti, A., Schwartz, J., Chen, J., Wu, T., Cohen, A., Gasparrini, A., and Kan, H.: Ambient Particulate Air Pollution and Daily Mortality in 652 Cities, N Engl J Med, 381, 705-715, https://doi.org/10.1056/NEJMoa1817364, 2019.

Liu, Q. and Schauer, J. J.: The oxidative potential of atmospheric particulate matter as an indicator of health risk of air pollution: a review, Environmental Chemistry Letters, 24, 229-250, https://doi.org/10.1007/s10311-025-01882-z, 2025.

Liu, Y. and Chan, C. K.: The oxidative potential of fresh and aged elemental carbon-containing airborne particles: a review, Environ Sci Process Impacts, 24, 525-546, https://doi.org/10.1039/d1em00497b, 2022.

Luan, M., Zhang, T., Li, X., Yan, C., Sun, J., Zhi, G., Shen, G., Liu, X., and Zheng, M.: Investigating the relationship between mass concentration of particulate matter and reactive oxygen species based on residential coal combustion source tests, Environ Res, 212, 113499, https://doi.org/10.1016/j.envres.2022.113499, 2022.

Luo, Y., Yang, X., Wang, D., Xu, H., Zhang, H., Huang, S., Wang, Q., Zhang, N., Cao, J., and Shen, Z.: Insights the dominant contribution of biomass burning to methanol-soluble PM(2.5) bounded oxidation potential based on multilayer perceptron neural network analysis in Xi'an, China, Sci Total Environ, 908, 168273, https://doi.org/10.1016/j.scitotenv.2023.168273, 2024.

Moller, P., Jacobsen, N. R., Folkmann, J. K., Danielsen, P. H., Mikkelsen, L., Hemmingsen, J. G., Vesterdal, L. K., Forchhammer, L., Wallin, H., and Loft, S.: Role of oxidative damage in toxicity of particulates, Free Radic Res, 44, 1-46, https://doi.org/10.3109/10715760903300691, 2010.

Nault, B. A., Canagaratna, M., Croteau, P., Fortner, E., Lambe, A. T., Stark, H., Sueper, D., Werden, B. S., Williams, A., Williams, L. R., Worsnop, D., Jayne, J., DeCarlo, P. F., Cubison, M., Papadopoulos, G., and Urs, R.: Characterization of a new higher-resolution time-of-flight aerosol chemical speciation monitor: Application for

https://doi.org/10.5194/egusphere-2026-6574
Preprint. Discussion started: 6 November 2026
© Author(s) 2026. CC BY 4.0 License.

measurements of atmospheric aerosols, Aerosol Science and Technology, 59, 719-742, https://doi.org/10.1080/02786826.2025.2481221, 2025.

Ng, N. L., Herndon, S. C., Trimborn, A., Canagaratna, M. R., Croteau, P. L., Onasch, T. B., Sueper, D., Worsnop, D. R., Zhang, Q., Sun, Y. L., and Jayne, J. T.: An aerosol chemical speciation monitor (ACSM) for routine monitoring of the composition and mass concentrations of ambient aerosol, Aerosol Science and Technology, 45, 780-794, https://doi.org/10.1080/02786826.2011.560211, 2011.

Nobile, F., Forastiere, A., Michelozzi, P., Forastiere, F., and Stafoggia, M.: Long-term exposure to air pollution and incidence of mental disorders. A large longitudinal cohort study of adults within an urban area, Environ Int, 181, 108302, https://doi.org/10.1016/j.envint.2023.108302, 2023.

Ovadnevaite, J., Lin, C., Rinaldi, M., Ceburnis, D., Buckley, P., Coleman, L., Facchini, M. C., Wenger, J., and O'Dowd, C. D.: Air Pollution Sources in Ireland, EPA IrelandEPA Research Report 385, 2021.

Pietrogrande, M. C., Bacco, D., Demaria, G., Russo, M., Scotto, F., and Trentini, A.: Polycyclic aromatic hydrocarbons and their oxygenated derivatives in urban aerosol: levels, chemical profiles, and contribution to PM(2.5) oxidative potential, Environ Sci Pollut Res Int, 29, 54391-54406, https://doi.org/10.1007/s11356-021-16858-z, 2022.

Pope, C. A. and Dockery, D. W.: Health effects of fine particulate air pollution: lines that connect, Journal of the Air & Waste Management Association, 56, 709-742, https://doi.org/10.1080/10473289.2006.10464485, 2012.

Price-Allison, A., Lea-Langton, A. R., Mitchell, E. J. S., Gudka, B., Jones, J. M., Mason, P. E., and Williams, A.: Emissions performance of high moisture wood fuels burned in a residential stove, Fuel, 239, 1038-1045, https://doi.org/10.1016/j.fuel.2018.11.090, 2019.

Puthussery, J. V., Zhang, C., and Verma, V.: Development and field testing of an online instrument for measuring the real-time oxidative potential of ambient particulate matter based on dithiothreitol assay, Atmospheric Measurement Techniques, 11, 5767-5780, https://doi.org/10.5194/amt-11-5767-2018, 2018.

Rinaldi, M., Manarini, F., Lucertini, M., Rapuano, M., Decesari, S., Paglione, M., Facchini, M. C., Lin, C., Ceburnis, D., D. O'Dowd, C., Buckley, P., Hellebust, S., Wenger, J., and Ovadnevaite, J.: Important Contribution to Aerosol Oxidative Potential from Residential Solid Fuel Burning in Central Ireland, Atmosphere, 15, 436, https://doi.org/10.3390/atmos15040436, 2024.

Schneider, E., Rüger, C. P., Chacón-Patiño, M. L., Somero, M., Ruppel, M. M., Ihalainen, M., Köster, K., Sippula, O., Czech, H., and Zimmermann, R.: The complex composition of organic aerosols emitted during burning varies between Arctic and boreal peat, Communications Earth & Environment, 5, https://doi.org/10.1038/s43247-024-01304-y, 2024.

Shen, D. K., Gu, S., Luo, K. H., Wang, S. R., and Fang, M. X.: The pyrolytic degradation of wood-derived lignin from pulping process, Bioresour Technol, 101, 6136-6146, https://doi.org/10.1016/j.biortech.2010.02.078, 2010a.

Shen, G., Xue, M., Wei, S., Chen, Y., Zhao, Q., Li, B., Wu, H., and Tao, S.: Influence of fuel moisture, charge size, feeding rate and air ventilation conditions on the emissions of PM, OC, EC, parent PAHs, and their derivatives from residential wood combustion, J Environ Sci (China), 25, 1808-1816, https://doi.org/10.1016/s1001-0742(12)60258-7, 2013a.

Shen, G., Tao, S., Chen, Y., Zhang, Y., Wei, S., Xue, M., Wang, B., Wang, R., Lu, Y., Li, W., Shen, H., Huang, Y., and Chen, H.: Emission Characteristics for Polycyclic Aromatic Hydrocarbons from Solid Fuels Burned in

https://doi.org/10.5194/egusphere-2026-6574
Preprint. Discussion started: 6 November 2026
© Author(s) 2026. CC BY 4.0 License.

Domestic Stoves in Rural China, Environmental Science & Technology, 47, 14485-14494, https://doi.org/10.1021/es403110b, 2013b.

Shen, G., Wang, W., Yang, Y., Zhu, C., Min, Y., Xue, M., Ding, J., Li, W., Wang, B., Shen, H., Wang, R., Wang, X., and Tao, S.: Emission factors and particulate matter size distribution of polycyclic aromatic hydrocarbons from residential coal combustions in rural Northern China, Atmos Environ (1994), 44, 5737-5743, https://doi.org/10.1016/j.atmosenv.2010.08.042, 2010b.

Shen, Y., Hu, Y., Wang, M., Bao, W., Chang, L., and Xie, K.: Speciation and thermal transformation of sulfur forms in high-sulfur coal and its utilization in coal-blending coking process: A review, Chinese Journal of Chemical Engineering, 35, 70-82, https://doi.org/10.1016/j.cjche.2021.04.007, 2021.

Simões, E. F. C., Almeida, A. S., Duarte, A. C., and Duarte, R. M. B. O.: Assessing reactive oxygen and nitrogen species in atmospheric and aquatic environments: Analytical challenges and opportunities, TrAC Trends in Analytical Chemistry, 135, https://doi.org/10.1016/j.trac.2020.116149, 2021.

Sun, Y., Du, W., Fu, P., Wang, Q., Li, J., Ge, X., Zhang, Q., Zhu, C., Ren, L., Xu, W., Zhao, J., Han, T., Worsnop, D. R., and Wang, Z.: Primary and secondary aerosols in Beijing in winter: sources, variations and processes, Atmospheric Chemistry and Physics, 16, 8309-8329, https://doi.org/10.5194/acp-16-8309-2016, 2016.

Tassel, C., Jaffrezo, J. L., Dominutti, P., Daellenbach, K. R., Darfeuil, S., Elazzouzi, R., Laj, P., Marsal, A., Mhadhbi, T., Dinh, V. N. T., Voiron, C., Houdier, S., Durif, M., Chatain, M., Francony, F., Cozic, J., Salque Moreton, G., Le Quilleuc, M., Ghersi, V., Gille, G., Mesbah, B., Stratigou, E., Zublena, M., Diemoz, H., Alastuey, A., D'Anna, B., Marchand, N., Conil, S., Gros, V., van Os, M. F., Salma, I., Mihalopoulos, N., Mocnik, G., Dzepina, K., Styszko, K., Huglin, C., Querol, X., Prevot, A. S. H., Favez, O., Siroux, V., and Uzu, G.: Oxidative potential of atmospheric particles in Europe and exposure scenarios, Nature, https://doi.org/10.1038/s41586-025-09666-9, 2025.

Trubetskaya, A., Lin, C., Ovadnevaite, J., Ceburnis, D., O'Dowd, C., Leahy, J. J., Monaghan, R. F. D., Johnson, R., Layden, P., and Smith, W.: Study of Emissions from Domestic Solid-Fuel Stove Combustion in Ireland, Energy Fuels, 35, 4966-4978, https://doi.org/10.1021/acs.energyfuels.0c04148, 2021.

Verma, V., Rico-Martinez, R., Kotra, N., King, L., Liu, J., Snell, T. W., and Weber, R. J.: Contribution of Water-Soluble and Insoluble Components and Their Hydrophobic/Hydrophilic Subfractions to the Reactive Oxygen Species-Generating Potential of Fine Ambient Aerosols, Environmental Science & Technology, 46, 11384-11392, https://doi.org/10.1021/es302484r, 2012.

Vernocchi, V., Brunoldi, M., Canepari, S., Corsini, E., Isolabella, T., Massimi, L., Mazzei, F., Melzi, G., Paglione, M., Pantaleoni, S., Prati, P., Rapuano, M., Rinaldi, M., Tiraboschi, C., and Massabo, D.: Oxidative potential and cellular toxicity of carbonaceous aerosols undergoing aging in an atmospheric simulation chamber, Toxicol Appl Pharmacol, 505, 117573, https://doi.org/10.1016/j.taap.2025.117573, 2025.

Wang, J., Jiang, H., Jiang, H., Mo, Y., Geng, X., Li, J., Mao, S., Bualert, S., Ma, S., Li, J., and Zhang, G.: Source apportionment of water-soluble oxidative potential in ambient total suspended particulate from Bangkok: Biomass burning versus fossil fuel combustion, Atmospheric Environment, 235, https://doi.org/10.1016/j.atmosenv.2020.117624, 2020.

Weimer, S., Alfarra, M. R., Schreiber, D., Mohr, M., Prévôt, A. S. H., and Baltensperger, U.: Organic aerosol mass spectral signatures from wood-burning emissions: Influence of burning conditions and wood type, Journal of Geophysical Research: Atmospheres, 113, D10304, https://doi.org/10.1029/2007JD009309, 2008.

https://doi.org/10.5194/egusphere-2026-6574
Preprint. Discussion started: 6 November 2026
© Author(s) 2026. CC BY 4.0 License.

Wilson, A. L., Cui, W., Hu, Y., Chiapasco, M., Rein, G., Porter, A. E., Fowler, G., and Stettler, M. E. J.: Particles emitted from smouldering peat: size-resolved composition and emission factors, Environ Sci Atmos, 5, 348-366, https://doi.org/10.1039/d4ea00124a, 2025.

Wragg, F. P. H., Fuller, S. J., Freshwater, R., Green, D. C., Kelly, F. J., and Kalberer, M.: An automated online instrument to quantify aerosol-bound reactive oxygen species (ROS) for ambient measurement and health-relevant aerosol studies, Atmospheric Measurement Techniques, 9, 4891-4900, https://doi.org/10.5194/amt-9-4891-2016, 2016.

Yang, H., Yan, R., Chen, H., Lee, D. H., and Zheng, C.: Characteristics of hemicellulose, cellulose and lignin pyrolysis, Fuel, 86, 1781-1788, https://doi.org/10.1016/j.fuel.2006.12.013, 2007.

Yun, X., Shen, G., Shen, H., Meng, W., Chen, Y., Xu, H., Ren, Y., Zhong, Q., Du, W., Ma, J., Cheng, H., Wang, X., Liu, J., Wang, X., Li, B., Hu, J., Wan, Y., and Tao, S.: Residential solid fuel emissions contribute significantly to air pollution and associated health impacts in China, Science Advances, 6, eaba7621, https://doi.org/10.1126/sciadv.aba7621, 2020.

Zhong, S., Liu, R., Yue, S., Wang, P., Zhang, Q., Ma, C., Deng, J., Qi, Y., Zhu, J., Liu, C. Q., Kawamura, K., and Fu, P.: Peatland Wildfires Enhance Nitrogen-Containing Organic Compounds in Marine Aerosols over the Western Pacific, Environ Sci Technol, 58, 10991-11002, https://doi.org/10.1021/acs.est.3c10125, 2024.

Zhou, J., Bruns, E. A., Zotter, P., Stefenelli, G., Prévôt, A. S. H., Baltensperger, U., El-Haddad, I., and Dommen, J.: Development, characterization and first deployment of an improved online reactive oxygen species analyzer, Atmospheric Measurement Techniques, 11, 65-80, https://doi.org/10.5194/amt-11-65-2018, 2018a.

Zhou, J., Zotter, P., Bruns, E. A., Stefenelli, G., Bhattu, D., Brown, S., Bertrand, A., Marchand, N., Lamkaddam, H., Slowik, J. G., Prévôt, A. S. H., Baltensperger, U., Nussbaumer, T., El-Haddad, I., and Dommen, J.: Particle-bound reactive oxygen species (PB-ROS) emissions and formation pathways in residential wood smoke under different combustion and aging conditions, Atmospheric Chemistry and Physics, 18, 6985-7000, https://doi.org/10.5194/acp-18-6985-2018, 2018b.

Zhou, W., Jiang, J., Duan, L., and Hao, J.: Evolution of Submicrometer Organic Aerosols during a Complete Residential Coal Combustion Process, Environ Sci Technol, 50, 7861-7869, https://doi.org/10.1021/acs.est.6b00075, 2016.